Vibrational spectrum renormalization by enforced coupling across the van der Waals gap between MoS_{2} and WS_{2} monolayers

Wen Fan, Xi Zhu, Feng Ke, Yabin Chen, Kaichen Dong, Jie Ji, Bin Chen, Sefaattin Tongay, Joel W. Ager, Kai Liu, Haibin Su, and Junqiao Wu

Phys. Rev. B **92**, 241408 — Published 18 December 2015

DOI: 10.1103/PhysRevB.92.241408

Vibrational spectrum renormalization across van der Waals gap by enforced inter hetero-bilayer coupling

Wen Fan[1*], Xi Zhu[2*], Feng Ke[3], Yabin Chen[1], Kaichen Dong[1], Jie Ji[4], Bin Chen[3], Sefaattin Tongay[5], Joel W. Ager[6], Kai Liu[7], Haibin Su[2], and Junqiao Wu[1,6]

1. Department of Materials Science and Engineering, University of California, Berkeley, CA 94720, U.S.A.

2. School of Materials Science and Engineering, Nanyang Technological University, Singapore 639798, Singapore

3. Center for High Pressure Science and Technology Advanced Research, Shanghai 201203,China

4. Department of Thermal Science and Energy Engineering, University of Science and Technology of China, Hefei, Anhui 230027, China

5. School of Engineering of Matter, Transport and Energy, Arizona State University, Tempe, AZ 85287, U.S.A.

6. Materials Sciences Division, Lawrence Berkeley National Laboratory, Berkeley, CA 94720, U.S.A.

7. School of Materials Science and Engineering, Tsinghua University, Beijing 100084, China

Abstract

At the few or monolayer limit, layered materials define an interesting two-dimensional system with unique electronic and phonon properties. The electron band structure of monolayers can be drastically different from multilayers despite the weak van der Waals interaction between neighboring layers. In this work, we demonstrate that vibrational spectra of a MoS_2 monolayer and a WS_2 monolayer are also renormalized when the interaction between them is artificially modulated. This is achieved by using a diamond anvil cell to apply high pressures, up to 39 GPa, onto WS_2/MoS_2 hetero-bilayers. With increasing pressure, the out-of-plane Raman frequencies of the two individual monolayers repel each other, exhibiting coherent vibrations across the van der Waals gap with an optical-like and an acoustic-like interlayer vibration mode. The discovery shows a crossover in lattice vibration from a two-dimensional system toward three-dimensional system driven by enforced interlayer coupling.

* These authors contribute equally to this work.

To whom correspondence should be addressed:

Prof. Junqiao Wu, wuj@berkeley.edu
Prof. Haibin Su, hbsu@ntu.edu.sg

In layered materials, strong intralayer covalent bonds and weak interlayer van der Waals (vdW) interactions allow for separation of single-crystalline layers via mechanical or chemical exfoliation.[1, 2] Although neighboring layers are held together by weak vdW interactions, physical properties of these layered semiconductors are sensitive to interlayer coupling across the vdW gap. For example, with a few exceptions (*e.g.*, ReS_2 [3]), many semiconducting transition metal dichalcogenides (*e.g.*, MoS_2, WS_2 and $MoSe_2$) switch from indirect bandgap in the bulk or multilayers to direct bandgap in the monolayer limit.[4-7] A few other layered semiconductors (*e.g.*, InSe) exhibit the opposite trend, *i.e.*, switching from direct bandgap in the bulk to indirect bandgap toward the monolayer limit.[8, 9] The normalization of band structure by the interlayer coupling signifies a crossover from two-dimensional (2D) electronic system in the monolayer to three-dimensional (3D) electronic system in the bulk. Therefore, the degree of two-dimensionality, or, the "2Dness", of the system is defined by the strength of interlayer coupling. If the interlayer coupling can be artificially reduced or enhanced, one can effectively modulate the electronic dimensionality of the system, which would offer much insight into low-dimensional physics. Indeed, this has been experimentally achieved with chemical intercalation or application of hydrostatic pressure. For instance, with the application of high hydrostatic pressures at 10 ~ 20 GPa, an insulator-metal phase transition with a rapid drop in resistivity has been observed in bulk MoS_2.[10-12]

These studies all focus on normalization of the electronic structure with artificially tuned interlayer coupling. It is less clear how the vibrational structure of the system responds to modulation of the interlayer coupling. In bulk or multilayer materials, their Raman active modes are found to stiffen with increasing pressure applied.[10-12] However, as the materials studied are composed of a stack of identical layers (hence homo-multilayers), it is not possible to distinguish the vibrational modes from individual monolayers. In this work, we apply high pressure to hetero-bilayers composed of a MoS_2 monolayer stacked on a WS_2 monolayer, and demonstrate that a dimensional crossover, similar to that observed in electronic band structure renormalization, occurs also in the lattice vibrational structure of the system.

We measured the Raman modes of the WS_2/MoS_2 hetero-bilayers, as well as separate MoS_2 and WS_2 monolayers, under hydrostatic pressure applied using a diamond anvil cell (DAC). The MoS_2 and WS_2 monolayers were grown by a well-established chemical vapor deposition (CVD) technique onto SiO_2/Si substrates.[13, 14] The WS_2/MoS_2 hetero-bilayers were prepared using polydimethylsiloxane (PDMS) stamping technique as described in previous reports.[14] Briefly, PDMS was spin coated on CVD grown monolayer $WS_2/SiO_2/Si$, and cured at 120 °C for >3 h. The PDMS/WS_2 was released from the SiO_2/Si substrate by mildly etching SiO_2 in 2 mol/L KOH solution for 0.5 ~ 2 h. It was then rinsed in DI water to remove the KOH residue, and transferred onto CVD grown monolayer $MoS_2/SiO_2/Si$ substrate, as shown in the Inset of Fig.1(a). Afterwards, the PDMS/WS_2/MoS_2 was released from the SiO_2/Si substrate by mild KOH etching again. It was then stamped onto the center of the diamond culet table of the DAC, and then the PDMS substrate was peeled off slowly, leaving the WS_2/MoS_2 hetero-bilayer on top of the diamond culet table. The sample was aligned to a small hole (diameter ~100 μm) drilled in a rhenium gasket and sealed by the two diamonds. The culet size of the diamonds is ~ 300 μm, and the gasket was pre-indented to a depth of ~ 40 μm to ensure good alignment and tight sealing. Hydrostatic pressure near the sample was determined by the standard ruby fluorescence method. The pressure medium used in our experiments was a mixture of methanol and ethanol (4:1). The

culet table was cleaned and wetted with the pressure medium prior to the sample stamping, to ensure existence of the medium between the sample and the culet surface. We note that the medium may freeze at pressures higher than ~10 GPa, which may result in slight inhomogeneities in pressure in the DAC. Raman spectroscopy was performed with a Renishaw micro-PL/Raman system using an excitation laser of wavelength 532 nm. The Raman spectra were recorded through the DAC with a laser spot size of ~2 μm in diameter, and an effective resolution of ~ 1 cm^{-1}. Over twenty samples were prepared and measured, all showing consistent results, with no difference seen between the two cases where MoS_2 is on top of WS_2 and the other way around, or between the pressure-loading and unloading processes.

For MoS_2 and WS_2 monolayers with the D_{3h} symmetry, there are two prominent Raman active modes, the in-plane E' mode and out-of-plane A_1' mode.[15] For naturally stacked homo-bilayers with D_{6h} symmetry, these two modes become the well-known E_{2g} and A_{1g} modes. For the WS_2/ MoS_2 hetero-bilayers, these modes are also represented here as E' and A_1'due to the same D_{3h} symmetry as in the monolayers. There are five different stacking patterns, AA1, AA3, AB1, AB2 and AB3 for such a bilayer, just like in the case of homo-bilayers.[16] For homo-multilayers, when the number of layers increases from monolayer, the out-of-plane A_1' mode shows stiffening while the E' mode shows softening. The former is due to enhancement in restoration force by interactions between the S atoms from neighboring layers; the latter is attributed to enhanced dielectric screening of long-range Coulomb interaction between the metal atoms (Mo or W), because different from the vibration involving only S atoms in the A_1' mode, in the E' mode the metal atoms also vibrate.[17, 18]

Typical Raman spectra of MoS_2 monolayer, WS_2 monolayer, and WS_2/MoS_2 hetero-bilayers at ambient pressure ($P \approx 0$) are shown in Fig. 1(b). The out-of-plane (A_1') and in-plane (E') Raman modes of MoS_2 and WS_2 are well resolved from their monolayers.[16] All four peaks are present in the WS_2/MoS_2 hetero-bilayers, and occur at positions identical to those of separate monolayers, indicating that the overlapped region is merely a mechanical stack of WS_2/MoS_2 bilayers without interlayer coupling. This is consistent with earlier reports that show negligible interaction between neighboring layers in as-stamped bilayers.[15-18]

Upon the application of high pressure, all four Raman peaks start to shift toward higher wavenumbers, accompanied with peak height reduction and width broadening. Some of the Raman spectra are selectively shown in Fig. 2(a), which compares hetero-bilayers and separate monolayers. The positions of these Raman peaks were determined by fitting the Raman spectra to a Lorentzian lineshape, and plotted in Fig. 2(b). We note that the data in Fig. 2(b) includes results recorded from multiple samples, as well as pressure loading/unloading. Two conclusions can be drawn from Fig.2(b): (I). The in-plane modes (E') vary with pressure linearly, while the out-of-plane modes (A_1') show a nonlinear pressure dependence; (II). More interestingly, the E' modes of hetero-bilayers exactly follow those of the separate monolayers, while the A_1' modes of hetero-bilayers deviate significantly from those of separate monolayers, showing a clear repelling behavior, *i.e.*, the stiffer A_1' mode ($A_1'(WS_2)_{hetero}$) is pushed up, while the softer A_1' mode ($A_1'(MoS_2)_{hetero}$) is pushed down. The fact that the E' modes of hetero-bilayers precisely follow those of the separate monolayers also provides independent validation of the measurements, ruling out possibility that the exotic pressure behavior of the A_1' modes was caused by pressure mis-calibration or sample degradation. The broadening of the peaks at high pressures may be partly caused by the inhomogeneities of pressure arising from solidification of

the pressure medium. The weak, broad peak between 450 and 500 cm^{-1} is possibly attributed to second order Raman modes.

To understand the pressure dependence of the Raman frequencies, we have carried out first-principles calculation of the system. All calculations were performed by density functional theory (DFT) using the DMol3 package.[19, 20] All electrons are included in the simulation and the Perdew- Burke-Ernzerhof (PBE) exchange-correlation functional with dispersion correction (PBE-D) was used.[21, 22] All the ions and cell parameters were fully relaxed until the force tolerance reaches 0.01 eV/Å with the applied external pressure. The Double Numerical plus polarization basis was used for convergence tests, and a centered Brillouin zone sampled at 24×24×5 was used for integration.

For calculation of the WS_2/MoS_2 hetero-bilayers, we sampled the five stacking patterns include AA1,AB1,AB3,AA3 and AB3.[16] The stacking energy trend is similar to homo-bilayer MoS_2,[16] *i.e.*, the AB1 and AA1 stackings are energy favorable than the others, and for the higher-energy cases (AB3 and AA3), the interlayer distance is larger. The stacking-dependent interlayer distance in WS_2/MoS_2 hetero-bilayers originates from the steric effect that a certain amount of space is needed between any two atoms to afford the energy cost of overlapping electron clouds, which is the same as that in the homo-bilayer MoS_2.

As the hetero-bilayers are randomly stacked in our experiments, we compare the experimental results with calculated results averaged by the five stacking patterns. Figure 2(c) shows the calculated, pressure-dependent A_1' and E' frequencies averaged by the five stacking patterns of the WS_2/MoS_2 hetero-bilayers, compared to those of the MoS_2 and WS_2 monolayers. First, we can see that the A_1' mode, which involves vibration of the S atoms only, is higher in WS_2 than in the MoS_2. The Bader charge analysis reveals that the S atom is -0.58e charged in WS_2 and -0.52e in MoS_2, and therefore the coulomb interaction is slightly stronger in WS_2, resulting in a higher A_1' mode frequency. This is also consistent with the higher cohesive energy of WS_2 (5.78 eV) than that of MoS_2 (5.18 eV).[23]

Our calculation of the A_1' modes of the WS_2/MoS_2 hetero-bilayers show that these modes vibrate separately when their distance is sufficiently large. However, when an external pressure is applied, the interlayer coupling is enhanced, such that the A_1' modes of the two layers turn into two coherent vibration modes, where S atoms in both the MoS_2 and WS_2 layer move in concert, one vibrating in phase and the other vibrating 180^o out-of-phase, respectively. The two S atoms from the two layers move along the opposite (same) direction in the coherent in-phase (out-of-phase) modes, leading to stiffened (softened) mode frequency compared to the original A_1' mode. In contrast, the in-plane E' modes in each layers are still uncoupled, even at high pressures, owing to their weak interlayer coupling.

We also found theoretically that the stacking pattern slightly affects the frequencies: for the AA3 and AB3 stackings,[16] the interlayer S-S atoms are head to head to each other, which makes the A_1' mode slightly more stiffener, about 3~4 cm^{-1} higher than the other stacking patterns. Since the E' modes are always decoupled between the two layers, there is no distinguishable difference for the E' modes between the various stacking patterns, as well as with the case of monolayers.

The pressure-induced mode stiffening can be understood from the Grüneisen parameter. The *i*th mode's Grüneisen parameter γ_i is computed by

$$\gamma_i = -\frac{V}{\omega_i}\frac{\partial \omega_i}{\partial V}, \qquad (1)$$

where V is the volume of the unit cell. The calculated γ values are $\gamma_{A_1'}^{MoS_2}$=1.2, $\gamma_{E'}^{MoS_2}$=1.8, $\gamma_{A_1'}^{WS_2}$=0.6 and $\gamma_{E'}^{WS_2}$=0.5, in good agreement with previous results.[24] Since γ_i is positive, the frequency ω_i will increases with reduced V caused by external pressure P, as observed in Fig 2 (a) and (b).

To better understand the vibrational spectrum normalization, we model the process with a weakly coupled harmonic oscillator system. As the lattice of the bilayer system is much stiffer in the plane than out of plane, the deformation effect from the hydrostatic pressure on the system can be considered as a uni-axial pressure applied in the out-of-plane direction. As shown in Fig. 3(a), the out-of-plane mode of the two separate monolayers (one for MoS_2 and the other for WS_2) is modelled by two separate harmonic oscillators vibrating at their eigen frequencies,

$$\omega_{1,2} = \sqrt{(k_{1,2} + 2k_{press})/m}, \qquad (2)$$

where $k_{1,2}$ is the intrinsic spring constant when the monolayers are free-standing, and k_{press} is the added stiffness of the spring constant by interactions of the monolayer at its two sides with the pressure medium, which is expected to increase with pressure. We note that as the A_1' mode involves vibration of the sulphur atoms only (Fig.1(b) Inset), the difference in the mass of cations (Mo and W) does not play a role in the discussion, and the effective mass m in Eq.(2) is set the same for ω_1 and ω_2. When a coupling with spring constant k_{int} is introduced between the two oscillators, the new eigen-frequencies ($\omega_\pm$) of the system are given by solving the coupled equation of motion,

$$\omega_\pm^2 = \frac{1}{2}(\omega_1^2 + \omega_2^2) + \omega_{int}^2 - \omega_{press}^2 \pm \frac{1}{2}\sqrt{(\omega_1^2 - \omega_2^2)^2 + 4\omega_{int}^4}, \qquad (3)$$

where $\omega_{int} = \sqrt{k_{int}/m}$ and $\omega_{press} = \sqrt{k_{press}/m}$. It can be seen that ω_+ and ω_- correspond to oscillation modes in which the two masses are vibrating in phase and 180° out of phase, akin to the conventional optical and acoustic phonon modes in a crystal, respectively. As a result, they are stiffened and softened, respectively, from the original frequencies (ω_1 and ω_2): $\omega_+ > \omega_1 > \omega_2 > \omega_-$. However, due to the difference between ω_{int} and ω_{press}, the amount of stiffening and softening are not equal to each other: $|\omega_+ - \omega_1| \neq |\omega_2 - \omega_-|$, which is evident from the experimental data in Fig.2(b). This is different from a conventional hybridization problem (*i.e.*, when $\omega_{int} = \omega_{press}$) in which the splitting in energy is expected to be symmetric. The fact that $|\omega_+ - \omega_1| < |\omega_2 - \omega_-|$ as seen in Fig. 2(b) suggests $\omega_{int} < \omega_{press}$, or $k_{int} < k_{press}$, *i.e.*, the interaction between the MoS_2 and WS_2 layers is weaker than that between the monolayer and the pressure medium.

In order to apply quantitatively this analytical model to our data, we assume, to the first order approximation, that both k_{int} and k_{press} rise linearly with pressure, such that $k_{int}/m = \beta_{int}P$ and $k_{press}/m = \beta_{press}P$, where β_{int} and β_{press} are two constants related to the Gruneisen parameter of these two interactions. Equation (3) is used to fit simultaneously to the pressure dependence of the two A_1' modes of WS_2/MoS_2 hetero-bilayers, as shown in Fig.3(b). In the fitting, the experimentally measured pressure dependencies of ω_1 and ω_2 of separate monolayers are directly used as input, and β_{int} and β_{press} are adjusted as the only fitting parameters. A least-square fitting to ω_+ and ω_- are shown in Fig.3(b), which yields β_{int}=625±50/cm^2-GPa and

β_{press}=825±50/cm^2-GPa. The strength of these interactions can be gauged by comparing to the intrinsic A_1' frequencies: at the maximum pressure ($P \sim 40$ GPa) attained in this study, the interlayer coupling k_{int} results in a significant shift in A_1' frequency by 158/cm, or ~ 39%. This large change is not surprising considering that the out-of-plane Young's modulus is estimated to be only ~ 7GPa for these van der Waals crystals.[25] Therefore, high pressure through the DAC is indeed a very effective means to modulate the interlayer coupling across the van der Waals gap, driving the crossover from a 2D vibrational (*i.e.*, interlayer decoupled) system toward an effectively 3D system (*i.e.*, coupled across neighboring layers).

We note that the modes ω_+ and ω_- in this hetero-bilayer system are in analogy to the A_{1g} (in-phase) and B_{1u} (out-of-phase) oscillation modes usually defined in homo-bilayers.[18] In the case of naturally AB-stacked homo-bilayers, however, the B_{1u} mode is Raman inactive forbidden by its symmetry.[18] In contrast, both ω_+ and ω_- are Raman active in our hetero-bilayers, due to relaxation of the symmetry rule by the random stacking configurations in the WS_2/MoS_2 hetero-bilayers. However, it is interesting to note the opposite trends of intensity of the ω_+ and ω_- peaks as seen in Fig.2(a): as pressure increases, the intensity of ω_+ is enhanced and that of ω_- is reduced. This can be attributed to a residual effect of the different degrees of Raman activity of the A_{1g} and B_{1u} modes in homo-bilayers. We also note that a similar mode repulsion has been observed in bulk InSe crystals under hydrostatic pressures below ~ 15GPa [26, 27]. However, we also note the difference: in our work we probe vibration in membranes of truly atomic thicknesses, and the repulsion in our work is between two identical modes, which is possible in our experiments because they are from MoS_2 and WS_2, respectively, and are thus spectrally distinguishable.

In conclusion, using a diamond anvil cell, the interlayer coupling between MoS_2 and WS_2 monolayers is mechanically modulated. As a result, the out-of-plane vibration of the system is strongly renormalized, resulting in two coherent vibration modes involving the sulphur atoms in the two monolayers to vibrate in and out-of-phase, respectively. The effect discovered here shows that the vibrational structure of layered materials can be artificially and reversibly modulated across the van der Waals gap, providing a means to probe dimensionality effects of 2D materials.

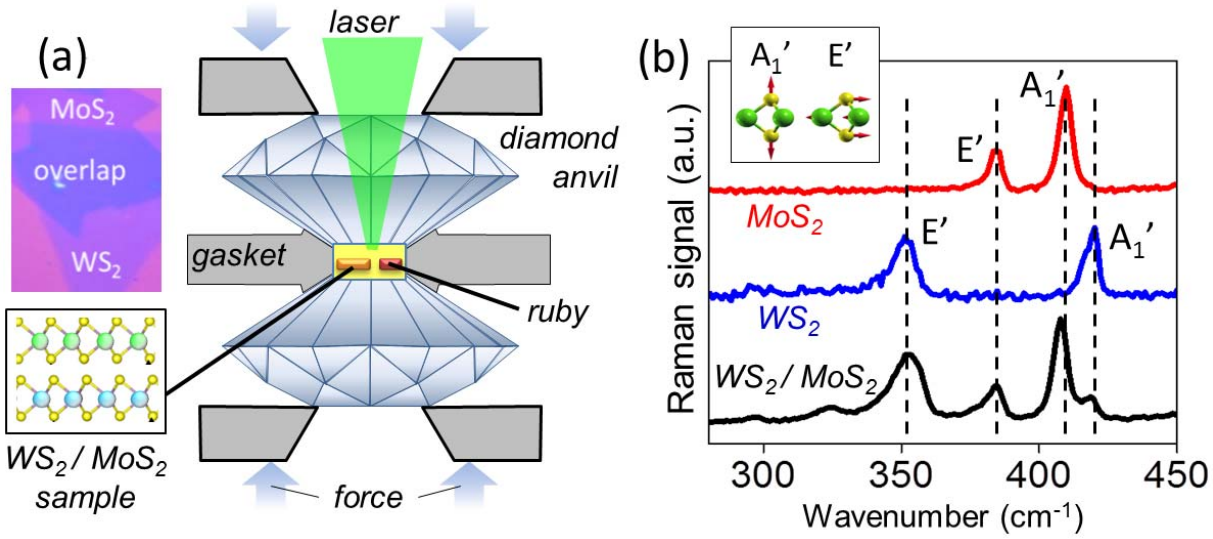

Figure 1 (a). Schematic of the high pressure experiment on WS_2/MoS_2 hetero-bilayers using a diamond anvil cell. Inset shows optical image of an overlapped region between MoS_2 and WS_2 monolayers on a SiO_x/Si surface (scar bar 10 μm). (b) Raman spectra of a MoS_2 monolayer, a WS_2 monolayer, and a WS_2/ MoS_2 bilayer recorded at ambient pressure ($P \approx 0$). The A_1' (out-of-plane) and E' (in-plane) peaks of each layer are labeled, and their oscillation modes are shown in the Inset.

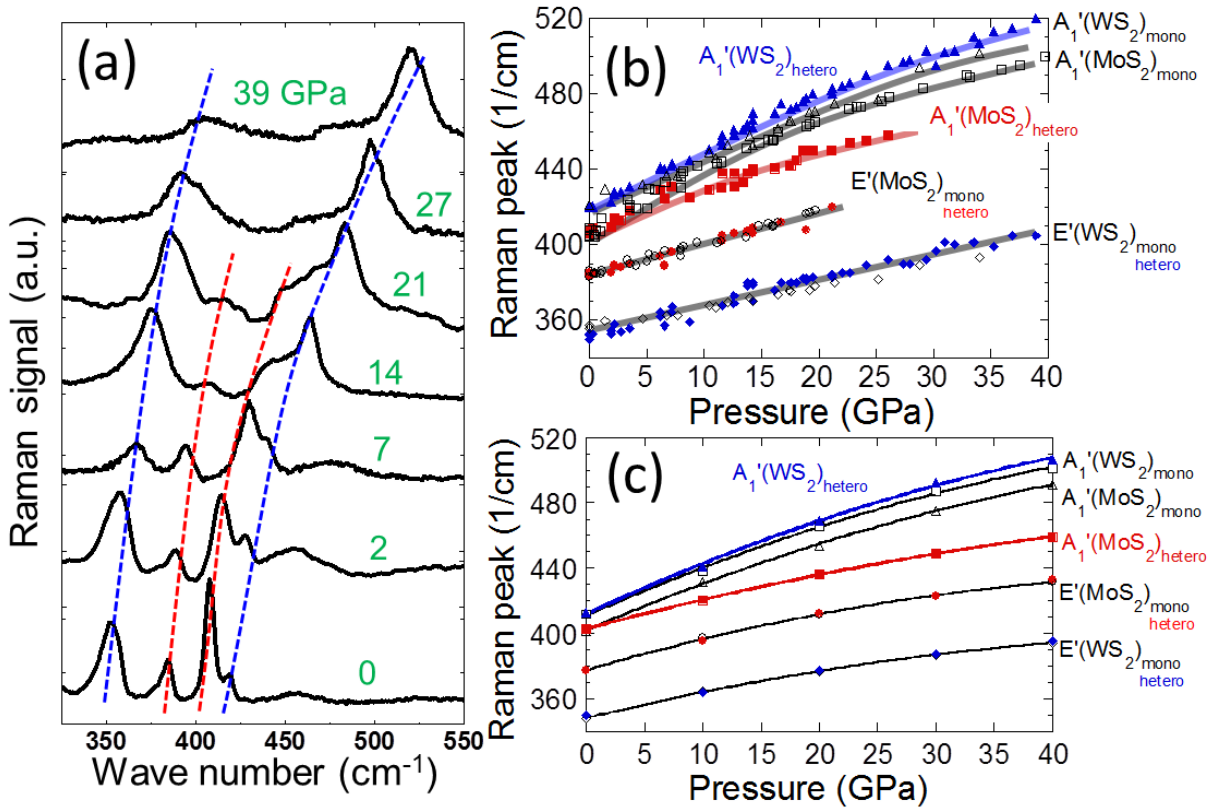

Figure 2 (a). Selected experimental Raman spectra recorded from a WS_2/MoS_2 hetero-bilayer at different pressures. Dashed lines are guide to the eye. (b). Raman peak positions of the A_1' and E' vibration modes as a function of pressure, color-coded by red (MoS_2 in hetero-bilayer), blue (WS_2 in hetero-bilayer) and black (both in monolayer). Lines are guide to the eye. It can be seen that the E' modes remain the same in bilayers as in monolayers, while the A_1' modes of MoS_2 and WS_2 in the bilayer are pushed away from each other. (c). Calculated pressure-dependent A_1' and E' modes in WS_2/MoS_2 bilayers averaged over five different stacking configurations. The calculated A_1' and E' modes of monolayer MoS_2 and WS_2 are also included as a comparison.

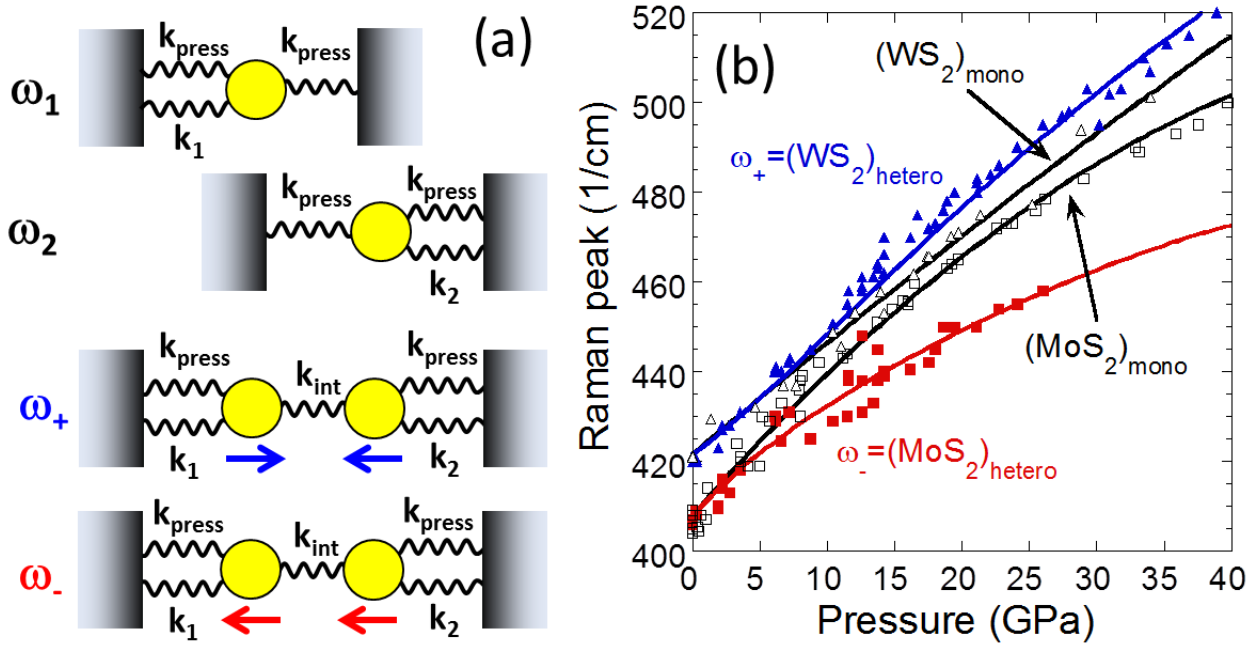

Figure 3. (a) Schematic of the model of two coupled harmonic oscillators, leading to two renormalized vibration frequencies ($\omega_{\pm}$) by enforced coupling (k_{int}). The arrows indicate the vibration directions for the coupled cases, representing the "optical-like" and "acoustic-like" modes for the coupled system. (b). Fitting to the measured A_1' frequencies in hetero-bilayers ($(WS_2)_{hetero}$, blue, and $(MoS_2)_{hetero}$, red) using the model in (a). The lines through the monolayer A_1' frequencies ($(WS_2)_{mono}$ and $(MoS_2)_{mono}$, black) are guide to the eye.

Acknowledgements:

This work was supported by the National Science Foundation under Grant No. DMR-1306601. H.S. is grateful for the hospitality from Dr. Jan Vasbinder in the Institute Para Limes in the early stage of this work. W.F. gratefully acknowledges Dr. Jinyuan Yan for help with the DAC setup, and Prof. Feng Wang for useful discussion. The laser milling was supported by COMPRES (EAR 11-57758). K.D. acknowledges the Chinese Scholarship Council (CSC, No. 201406210211) for financial support. J.W., J.W.A. and Y.C. acknowledge support from the Singapore-Berkeley Research Initiative for Sustainable Energy (SinBeRISE).

References

1 Q. H. Wang, K. Kalantar-Zadeh, A. Kis, J. N. Coleman, and M. S. Strano, Nature Nanotech. 7, 699 (2012).

2 A. K. Geim and I. V. Grigoriev, Nature 499, 419 (2013).

3 Sefaattin Tongay, Hasan Sahin, Changhyun Ko, Alex Luce, Wen Fan, Kai Liu,Jian Zhou, Ying-Sheng Huang, Ching-Hwa Ho, Jinyuan Yan, D. Frank Ogletree, Shaul Aloni, Jie Ji, Shushen Li, Jingbo Li, F. M. Peeters, and Junqiao Wu, Nature Commun. 5, 3252 (2014).

4 K. Mak, C. Lee, J. Hone, J. Shan, and T. F. Heinz, Phys. Rev. Lett. 105, 136805 (2010).

5 K. F. Mak, K. He, C. Lee, G. H. Lee, J. Hone, T. F. Heinz, and J. Shan, Nature Mater. 12, 207 (2012).

6 A. Splendiani, L. Sun, Y. Zhang, T. Li, J. Kim, C. Y. Chim, G. Galli, and F. Wang, Nano Lett. 10, 1271 (2010).

7 S. Tongay, J. Zhou, C. Ataca, K. Lo, T. S. Matthews, J. Li, J. C. Grossman, and J. Wu, Nano Lett. 12, 5576 (2012).

8 Garry W. Mudd, Simon A. Svatek, Tianhang Ren, Amalia Patanè, Oleg Makarovsky, Laurence Eaves, Peter H. Beton, Zakhar D. Kovalyuk, George V. Lashkarev, Zakhar R. Kudrynskyi, and Alexandr I. Dmitriev, Adv. Mater. 25, 5714 (2013).

9 Sidong Lei, Liehui Ge, Sina Najmaei, Antony George, Rajesh Kappera, Jun Lou, Manish Chhowalla, Hisato Yamaguchi, Gautam Gupta, Robert Vajtai, Aditya D. Mohite, and Pulickel M. Ajayan, ACS Nano 8, 1263 (2014).

10 Avinash P. Nayak, Tribhuwan Pandey, Damien Voiry, Jin Liu, Samuel T. Moran, Ankit Sharma, Cheng Tan, Chang-Hsiao Chen, Lain-Jong Li, Manish Chhowalla, Jung-Fu Lin, Abhishek K. Singh, and Deji Akinwande, Nano Lett. 15, 346 (2015).

11 Z. H. Chi, X. M. Zhao, H. Zhang, A. F. Goncharov, S. S. Lobanov, T. Kagayama, M. Sakata, and X. J. Chen, Phys. Rev. Lett. 113, 036802 (2014).

12 Avinash P. Nayak, Swastibrata Bhattacharyya, Jie Zhu, Jin Liu, Xiang Wu, Tribhuwan Pandey, Changqing Jin, Abhishek K. Singh, Deji Akinwande, Jung-Fu Lin, Nature Commun. 5, 3731 (2014).

13 Yi-Hsien Lee, Xin-Quan Zhang, Wenjing Zhang, Mu-Tung Chang, Cheng-Te Lin, Kai-Di Chang, Ya-Chu Yu, Jacob Tse-Wei Wang, Chia-Seng Chang, Lain-Jong Li and Tsung-Wu Lin, Adv. Mater. 24, 2320 (2012).

14 Sefaattin Tongay, Wen Fan, Jun Kang, Joonsuk Park, Unsal Koldemir, Joonki Suh, Deepa S. Narang, Kai Liu, Jie Ji, Jingbo Li, Robert Sinclair, and Junqiao Wu, Nano Lett. 14, 3185 (2014).

15 C. Lee, H. Yan, L. E. Brus, T. F. Heinz, J. Hone, and S. Ryu, ACS Nano. 4, 2695 (2010).

16 Kaihui Liu, Liming Zhang, Ting Cao, Chenhao Jin, Diana Qiu, Qin Zhou, Alex Zettl, Peidong Yang, Steve G. Louie and Feng Wang, Nature Commun. 5, 4966 (2014).

17 Philipp Tonndorf, Robert Schmidt, Philipp Böttger, Xiao Zhang, Janna Börner, Andreas Liebig, Manfred Albrecht, Christian Kloc, Ovidiu Gordan, Dietrich R. T. Zahn, Steffen Michaelis de Vasconcellos, and Rudolf Bratschitsch, Opt. Express 21, 4908 (2013).

18 A. Molina-Sanchez and L. Wirtz, Phys. Rev. B 84, 155413 (2011).

19 B. Delley, J. Chem. Phys. 92, 508 (1990).

20 B. Delley, J. Chem. Phys. 113, 7756 (2000).

21 S. Grimme, J. Comput. Chem. 27, 1787 (2006).

22 J. P. Perdew, K. Burke, and M. Ernzerhof, Phys. Rev. Lett. 77, 3865 (1996).

23 P. Raybaud, G. Kresse, J. Hafner, and H. Toulhoat, J. Phys.: Condens. Matter 9, 11085 (1997).
24 Y. Ding and B. Xiao, RSC Adv. 5, 18391 (2015).
25 D. Fu, J. Zhou, S. Tongay, K. Liu, W. Fan, T.-J. King, and J. Wu, Appl. Phys. Lett. 103, 183105 (2013).
26 In-Hwan Choi and Peter Y. Yu, Phys. Rev. B 68, 165339 (2003).
27 D. Errandonea, D. Martínez-García, A. Segura, J. Haines, E. Machado-Charry, E. Canadell, J. C. Chervin, and A. Chevy, Phys. Rev. B 77, 045208 (2008).